Comprehensive Analysis of Human Subtelomeres by Whole Genome Mapping

Eleanor Young[1], Heba Z. Abid[1], Pui-Yan Kwok[2,3,4], Harold Riethman[5§], Ming Xiao[1,6,§]

[1]School of Biomedical Engineering and [6]Institute of Molecular Medicine and Infectious Disease in the School of Medicine, Drexel University, Philadelphia, PA

[2]Cardiovascular Research Institute, [3]Department of Dermatology, and [4]Institute for Human Genetics, University of California–San Francisco, San Francisco, CA

[5] Medical Diagnostic & Translational Sciences, Old Dominium University, Norfolk, VA

[§]Corresponding authors: Harold Riethman (hriethma@odu.edu), Ming Xiao (Ming.Xiao@drexel.edu)

Abstract:

Detailed comprehensive knowledge of the structures of individual long-range telomere-terminal haplotypes are needed to understand their impact on telomere function, and to delineate the population structure and evolution of subtelomere regions. However, the abundance of large evolutionarily recent segmental duplications and high levels of large structural variations have complicated both the mapping and sequence characterization of human subtelomere regions. Here, we use high throughput optical mapping of large single DNA molecules in nanochannel arrays for 154 human genomes from 26 populations to present a comprehensive look at human subtelomere structure and variation. The results catalog many novel long-range subtelomere haplotypes and determine the frequencies and contexts of specific subtelomeric duplicons on each chromosome arm, helping to clarify the currently ambiguous nature of many specific subtelomere structures as represented in the current reference sequence (HG38). The organization and content of some duplicons in subtelomeres appear to show both chromosome arm and population-specific trends. Based upon these trends we estimate a timeline for the spread of these duplication blocks.

Author Summary:

The ends of human chromosomes have caps called telomeres that are essential. These telomeres are influenced by the portions of DNA next to them, a region known as the subtelomere. We need to better understand the subtelomeric region to understand how it impacts the telomeres. This subtelomeric region is not well described in the current references. This is due to large variations in this region and portions that are repeated many times, making current sequencing technologies struggle to capture these regions. Many of these variations are evolutionary recent. Here we use 154 different samples from the 26 geographic regions of the world to gain a better understanding of the variation in these regions. We found many new

haplotypes and clarified the haplotypes existing in the current reference. We then examined population and chromosome specific trends.

Introduction:

Telomere-adjacent DNA helps regulate telomere (TTAGGG)n tract lengths and telomere integrity. A family of long noncoding telomeric repeat-containing RNA (TERRA) molecules is transcribed from subtelomeres into (TTAGGG)n tracts (1-3), and association of TERRA with other shelterin components and telomeric DNA is necessary for telomere integrity and function (1, 4, 5). Subtelomeric DNA elements cis to (TTAGGG)n tracts regulate both TERRA levels and haplotype-specific (TTAGGG)n tract lengths and stabilities (4, 6-9) with evidence for epigenetic modulation of these effects (9-12). Extended subtelomere regions contain both coding and non-coding transcripts, the abundance and regulation of which are likely to depend upon the specific haplotypes and copy number of the DNA encoding them. Some of these transcripts such as those encoding human WASH proteins are clearly functional, but most are not well-characterized (13-17). *De novo* deletion of specific subtelomeric duplications can cause disease in some contexts (18). Long-range interactions of telomeres with functional subtelomeric genes has been observed, with the expression of these genes sometimes regulated in a telomere length-dependent fashion (19, 20).

Large structural variations occur frequently in subtelomeric DNA, often associated with loss or gain of large pieces of evolutionarily recent segmental duplications. Ambiguities in sequence localization because of segmental duplication content, as well as the presence of alternative haplotypes differing by relatively large insertions, deletions, and more complex sequence organization differences, have contributed to gaps and misassemblies in subtelomeric regions of the human reference sequence. In the current version (HG38) single haplotypes of many subtelomeres have been sequenced to the beginning of terminal repeat (TTAGGG)n tracts, whereas others still contain (TTAGGG)n-adjacent gaps. These ambiguities are

represented in HG38 as strings of unknown nucleotides ("NNN's") intended to represent stretches of DNA with the number of "NN's" corresponding to estimated basepair (bp) length of the gap from the existing subtelomeric reference to the end of each respective chromosome arm (21, 22).

These ambiguities in the reference sequence, along with knowledge gained from limited long-range mapping studies that many additional large subtelomeric structural variations likely remain to be characterized (23), make the routine use of subtelomeric reference sequences problematic. Stong et al. (24) updated subtelomeric assemblies by using telomere clones from a fosmid structural variation resource(25) to fill in relatively small (TTAGGG)n-adjacent sequence gaps in the clone-based reference sequence, and re-defined subtelomere coordinates that exclude the (TTAGGG)n tract itself in order to create a custom subtelomere reference assembly ("Stong Assembly") useful for characterizing subtelomeric segmental duplications and extending the subtelomere paralogy blocks originally defined by Trask and co-workers (26). This resulted in an assembly significantly more useful for subtelomere characterization and short-read sequence mapping purposes than previous ones; subtelomeres were operationally defined as the distal 500 kb regions of each chromosome arm, and encompassed all known multi-telomere segmental duplications (Subtelomere Repeat Elements, SREs). The SREs comprise roughly 25 % of the entire subtelomere region and 80 % of the most distal 100 kb of these regions; each defined subtelomere region also contained a stretch of 1-copy subtelomere-specific DNA on its centromeric end that definitively connects it with the rest of the reference sequence (24). The improved subtelomere assemblies are still subject to ambiguities associated with a few remaining large telomere-adjacent gaps as well as many very large structural variations that define alternative long-range haplotypes for an unknown number of individual subtelomeres in human populations.

We have previously used single-molecule optical mapping to identify long-range haplotypes in human genomes (27, 28), and showed that long (average 300kb) molecules

92 mapped using this procedure can span segmental duplications in subtelomeres and connect
93 chromosome ends to 1-copy arm-specific DNA (22). Here we extend our analyses using high
94 throughput optical mapping of large single DNA molecules in nanochannel arrays for 154
95 human genomes from 26 populations to present a comprehensive look at human subtelomere
96 structure and variation. The results catalog many novel long-range subtelomere haplotypes and
97 determine the frequencies and contexts of specific subtelomeric duplicons on each
98 chromosome arm, helping to clarify the currently ambiguous nature of many specific
99 subtelomeres as represented in the current reference sequence (HG38).
100
101 **Results:**
102 **Individual subtelomeric consensus maps containing large SRE regions**
103 Subtelomeric repeat element (SRE) regions are located in the most distal stretches of human
104 subtelomeres. Long SRE regions of about 300 kb have been identified in some alleles of the 1p,
105 8p and 11p telomeres, whereas 7 telomeres have minimal or no SRE content (17, 24, 29, 30).
106 Most SRE regions are 40–150 kb in size (24). Physical linkage of 1-copy regions with telomeres
107 on single large DNA molecules capable of spanning SRE regions is required for assembling
108 individual subtelomeric consensus maps. Recently-developed high-throughput single-molecule
109 genome mapping methods are well-suited for this challenge. In this method, genomic DNA is
110 labeled at sites recognized by a sequence motif-specific Nicking endonuclease, long genomic
111 DNA fragments are isolated and imaged in nanochannel arrays to a high depth of coverage and
112 contigs of these large genomic DNA fragments are assembled from these data. In our case, these
113 maps are then compared with in silico-generated maps of subtelomeric reference sequences. Fig
114 1 shows the consensus map (yellow) and constituent single-molecules (brown) of the 3q
115 subtelomere from the GM191025 genome aligned with HG38 reference (blue) and the 3q
116 assembly from Stong et al. (2014; top). The paralog blocks of SREs are shown in the colored
117 rectangles defined in Stong et al. (2014). The long DNA molecules shown here are at least

0.35Mb, reaching into the single copy region of the 3q arm. Their good alignment in the single copy region indicates these molecules belong to 3q. These molecules also contain 130 kb of extra sequences beyond the end of the incomplete HG38 reference and Stong et al. assembly; the nicking pattern of this extra sequence is consistent with paralogy blocks 1-5 as shown (dashed boxes on top of the molecules in Fig. 1)**.** The GM191025 genome map indicates there is 130 kb of DNA extending beyond the end of the HG38 reference sequence (teal arrow), including 60 kb accounted for by the gap sequence (black arrow). All of this additional DNA is associated with previously-identified SRE paralogy blocks.

Discovery of novel subtelomeric structural variants, resolution of sequence gaps and delineation of long-range subtelomeric haplotypes across 154 genomes.

To gain better insight into the subtelomeric regions, we next analyzed genome maps of subtelomeric regions of 154 human genomes selected from the 1000 genome project (31). These genomes include 3 males and 3 females from each of the 26 ethnic regions of the world. By using this large and diverse sample set, we hope to form a more accurate representation of haplotypes and variations found in the subtelomeric regions of all chromosome arms.

Highly Variable Subtelomeres. Out of 46 chromosome arms, 18 (1p, 2q, 3q, 5q, 6p, 6q, 7p, 7q, 8p, 9p, 9q, 11p, 14q, 15q, 16q, 17q, 19p, 20p) are classified as highly variable. These are arms where structurally variant haplotypes were found in more than 10% of the total genomes analyzed (22) . Fig 2 (A, B, C, D, E, F) summarizes the distribution of haplotypes for each of these highly variable chromosome arms. The consensus maps of these subtelomeric regions show a wide range of variation between genomes, most strikingly in the length and sequence content of sequence content of telomere-adjacent DNA segments. In many cases (1p, 6p, 7p, 9q, 11p, 16q, 19q, 20p), the HG38 reference doesn't represent the main haplotype. Fig 2 follows the same convention as in Fig 1, except the black dashed arrow signifies that a region of telomere-adjacent gap sequence in the HG38 reference should be deleted. A red 'T' indicates the Stong assembly reached the telomere sequences for that arm.

1p: For 96 genomes the chromosome starts near the 0.6Mb coordinate of the HG38 reference chromosome 1p arm, and for another 17 genomes it starts around 0.5Mb of the hg38 reference. The remaining 41 genomes failed to assemble. There are no perfectly aligned contigs between 0-0.5Mb of the HG38 reference. We confirmed this using an alternative labeling method, direct label enzyme (DLE; 33). In a separate study of 6 genomes, we tagged the telomeres with CRISPR-cas9, and found that all molecules in these genomes containing telomeres align to the hg38 reference starting at 0.6Mb (31, 32). Fig 3 contains an example of one of these telomere images. This indicates that the first 500kb in hg38 reference for chromosome 1p contains incorrectly mapped DNA; indeed, analysis of DNA from each of the sequenced clones from this 500 kb region indicate that it is comprised entirely of segmental duplications, explaining its incorrect mapping location.

2q: For 2q, there is a major haplotype with 110 genomes that matches well to the hg38 reference. 20 genomes have an extension 45 kb more than the hg38 reference end. This is very similar in size to a 50 kb polymorphism at 2q detected independently using RARE cleavage mapping (33). 3 genomes start at 242.12Mb, and DNA from the remaining 21 genomes failed to assemble a contig at this telomere.

3q: 72 genomes extend 130 kb beyond the Stong assembly and hg38 reference as shown for GM191025 (Fig 1). The genome map pattern of this region indicates that these genomes contain paralogy blocks 1-5, which are lacking in both the hg38 reference and the Stong Assembly (4). 5 genomes extend an additional 70 kb and contains paralogy blocks 23, 24, 25 and 28. Another 10 genomes contain variable extensions beyond the reference, and 23 genomes start at 198.16 Mb. DNA from 44 genomes failed to assemble a contig at this telomere.

5q: 135 genomes start at 181.48 Mb. 116 out of the 135 genomes match the hg38 reference and 19 genomes of 135 genomes have alternative patterns in the last 30kb adjacent

to telomere. An additional 15 genomes start before 181.48Mb. None of these genomes contain 181.48Mb-181.54Mb telomere adjacent gap Ns (the black dash arrow in Fig. 2), which should be deleted from the hg38 reference. DNA from 4 genomes failed to assemble a contig at this telomere.

6p: 69 genomes start near 0.05 Mb of the HG38 reference sequence and the patterns from 0.05Mb to 0.11Mb are significantly different to hg38. 50 genomes start at 0.0 Mb of hg38. Most of the 50 genomes contain additional paralogy block 1-3, and 20 such genomes are shown in Fig. 2. DNA from 35 genomes failed to assemble a contig at this telomere...

6q: 80 genomes match the hg38 reference. 66 genomes have different variations between 170.74-170.70Mb. One specific pattern containing 15 genomes is shown in Fig. 2. All of these haplotypes start near the 170.75 Mb of hg38 reference sequence, and do not contain the 60 kb telomere-adjacent gap Ns in the HG38 reference sequence. DNA from 8 genomes failed to assemble a contig at this telomere.

7p: The 7p subtelomeric region shows a wide range in haplotypes, and all contain extra sequences beyond the hg38 reference. 60 genomes contain 70kb extra sequences, which have the patterns of paralogy blocks of 6-7-8-9. An additional 5 contain 175 kb extra sequences, which comprise of paralogy blocks from 1 to 9, as shown in Fig. 2. 39 genomes contain variable extensions beyond hg38. DNA from 50 genomes did not generate complete assembly due to an INP site, starting at 0.08Mb.

7q: 125 genomes match the HG38 reference pattern exactly or have one extra nick site. 17 genomes have 2 additional nick sites and extend 15 kb further than the major haplotype. DNA from the remaining 12 genomes failed to assemble a contig at this telomere.

8p: 104 genomes contain the major haplotype that matches the hg38 reference, stopping just before the telomere-adjacent gap Ns in HG38 that begin at 0.06Mb. 38 genomes start at 0.16Mb beginning with block 5 (lacking blocks 24, 25, 28, 19ab, 20 and 4). 11 genomes are the same length as the major haplotype but a different sequence composition for the last

196 0.09Mb. A set of 3 genomes (sharing one haplotype) out of 11 genomes containing blocks 1, 2,
197 3 and 4 (but having alternate nicking patterns relative to the set of 3) are shown in Fig. 2.
198 **9p**: 110 genomes have a haplotype that agrees well with the HG38 reference. 20
199 genomes have an extended region of 15kb with an unknown block, while 6 genomes have a
200 much longer extended region (60kb of beyond the HG38 reference also unknown block). DNA
201 from the remaining 18 genomes failed to assemble a contig at this telomere.
202 **9q:** 51 genomes extend 80kb beyond its distal end of hg 38 reference with blocks 3, 4
203 and some unknown sequence as well. 77 genomes extend into the 60kb telomere adjacent gap
204 Ns of hg38 reference. 15 of these 77 genomes shown in Fig.2 match until 138.3Mb and have an
205 unknown block for their last 30kb region.
206 **11p**: 11p is highly variable. 41 genomes shown in Fig.2 extend 90kb beyond the
207 telomere-adjacent gap boundary in HG38 reference and contain blocks 1,2,3,4. 80 genomes
208 show variable extension into the 60kb telomere gap Ns. 20 genomes among this group extend
209 0.11Mb from the telomere before matching the HG38 reference pattern and are shown in Fig 2.
210 **14q**: 95 genomes end at 106.7Mb and do not extend into the telomere gap adjacent Ns.
211 61 of these genomes have minor differences from the other 34 genomes in the region 106.7Mb
212 to 106.75Mb and in 106.85Mb to 106.86Mb region as seen in Fig. 2. This region is known to
213 contain variable genes from the immunoglobulin G heavy chain cluster (34). DNA from the
214 remaining 59 genomes failed to assemble a contig at this telomere.
215 **15q**: 114 genomes match well to the reference. 25 genomes are the same length but
216 have variation from 101.95-101.97Mb. Our previous work (22) revealed what turns out to be a
217 very rare haplotype of 15q with a 50kb extension. Only one genome in the current dataset
218 matched that particular haplotype and it was identical to one from the prior study (GM12892).
219 DNA from 14 genomes failed to assemble a contig at this telomere.
220 **16q**: 73 genomes match the HG 38 reference sequence length and extend only 0.02Mb
221 into the telomere adjacent gap Ns. These match the Stong et al. (2014) 16q assembly. An

additional 48 genomes extend around 0.08Mb into the telomere adjacent gap Ns with several variations in this extension. As shown in Fig 2, 3 of these genomes also differ from the reference at 90.18Mb-90.23Mb and contains blocks 1, 2,3,4,5. Another 5 of these extended genomes match the reference but still include blocks 1, 2, 3, 4. DNA from 33 genomes failed to assemble a contig at this telomere.

17q: 105 genomes have a haplotype matching the reference. 19 genomes have a similar pattern but 83.22-83.24 contains variation. Fig 2 shows one example of this group with 3 genomes. DNA from 30 genomes failed to assemble a contig.

19p: 62 genomes share a haplotype that matches the end of the reference sequence but is different from that reference at 0.12-0.2Mb, lacking block 5. 44 genomes match the reference and contain block 5. 10 of these 44 genomes extend 0.02Mb into the telomere adjacent gap Ns. DNA from 13 genomes have an 80kb extension with unknown blocks, exceeding the length of the telomere-adjacent gap Ns in the HG38 reference, 3 with the same variation from the reference at 0.12-0.2Mb. Fig 2 shows the 10 that extend and matches block 5 at 0.12Mb. 35 genomes failed to assemble.

20p: All of the 135 genomes in 20p extend beyond the 60kb telomere-adjacent gap Ns (black arrow). 94 genomes extend 0.1Mb, 41 genomes extend 0.14Mb (with the distal 0.09Mb differing). DNA from 19 genomes failed to assemble a contig at this telomere.

Subtelomeres with minimal structural variation. 18 chromosome arms (1q, 2p, 3p, 4p, 4q, 5p, 8q, 10p, 10q, 11q, 12p, 12q, 13q, 18p, 18q, 20q, 21q, XqYq) show minimal structural variation compared to the HG38 reference. Descriptions and figures depicting these arms can be found in the supplementary materials, Figs S1 to S7. Among these arms, inconsistencies with the current HG38 reference included 20 kb of extra gap DNA adjacent to the telomere at 8q of the HG38 reference, 110 kb of gap DNA adjacent to 18q of the HG38 reference, and 70 kb of extra gap DNA at 20q of the HG38 reference.

The current HG38 reference does not contain information on the p arms of the acrocentric chromosomes, 22p, 21p, 13p, 14p, and 15p, and thus could not be mapped to our single-molecule assemblies. However, in our recent study, genome maps pick up significant patterns of these acrocentric short-arm subtelomeres (31). For the XpYp, only a few genomes had contigs matching part of this region. They have similar patterns but variable spacing between the patterns (S6), and are located centromeric to a large hypervariable pseudoautosomal VNTR that has been associated with length polymorphisms up to 100 kb that would be expected to interfere with reference sequence assembly (34, 35).

Four subtelomeres (16p, 17p, 19q and 22q) have known inverted nick pair (INP) sites near the telomere with Nt.BspQ1 labeling, such that the genome maps can't extend to the telomeres. INP sites occur where the nicking enzymes sites are close together on opposing strands, leading to double stranded DNA breaks and thus interference with nick-label mapping.

We further characterized these 4 arms with DLE labeling (36) using a subset of genomes. The DLE enzyme does not nick the DNA, and intact molecules from this analysis confirmed the presence of INP sites using the nicking method. Based on this data, 19q and 22q show minimal variations and align well to the hg38 reference. 16p appears to have at least a second longer haplotype as suggested by some of the Nt.BspQ1 genomes, and they also had a longer minor haplotype shown with DLE. The existence of these structurally variant haplotypes is consistent with early PFGE mapping studies showing large subtelomeric polymorphisms at 16p (37). Genomes labeled with the DLE enzyme showed large differences between mapping patterns for 17p compared with the HG38 reference and further characterization will be needed to accurately classify this arm. Previous 17p subtelomere mapping and sequencing studies showed several discrete large tandem repeat regions within 100 kb of the chromosome end based upon a telomere-containing half-YAC as well as large variations detected by RARE cleavage(30, 38). Both 17p features may be contributing to difficulties characterizing this subtelomere in the population. The DLE method also mapped very few contigs to arm XpYp,

only 10 out of 52 genomes, suggesting, as mentioned above, that the reference may be inaccurate or XpYp may be highly variable with the reference only reflecting one haplotype.

It is clear that the existing human genome reference (hg38) for highly variable subtelomeric regions is often incomplete, especially in the region immediately adjacent to telomere repeats. The uncertainty is often expressed in telomere-adjacent gap regions ranging from 5-160kb on the end of these chromosome arms in the hg38 reference, and these gap sizes correlate poorly with the actual sizes of the structurally variant alleles...

In some cases, we confirmed that extra genomic materials should be added to the end of some arms, such as 2q, 3q, 7p, 9p, 9q, 11p, 19p, and 20p, which can be easily verified by the extra genome map extensions (teal arrow in fig. 2 and supplementary fig. S1-S7). In other cases, none of the genome maps extend across these telomere-adjacent gaps, which suggests that the regions should be deleted. To further confirm the inaccuracy of specific telomere-adjacent gaps in HG38, we used CRISPR-Cas9 to label the telomere to indicate the end of the genome maps. Fig 3 shows the typical results of this analysis for chromosome arms 1p, 3q, 8p, 14q, and 18q. The raw images of single DNA molecules were shown below the hg38 reference map (blue bar) and consensus genome map (yellow bar). For 8p, the green dots (Nt.BspQ1 motifs) on the blue DNA backbone align really well with the reference map and consensus map. At the end of the molecule, telomeres are shown as a more intense green dot, which was labeled with CRISPR cas9 (32) . Without the CRISPR-cas9 labeling, molecules with the same nick site pattern lack the intense green end labels. This confirms that the approximately 60kb telomere-adjacent gap in the telomere-adjacent region of 8p is inaccurate. A similar conclusion can be drawn for 14q (160kb) and 18q (110kb). As discussed earlier the 1p reference appears inaccurate and contigs start much further toward the centromere. This is confirmed by the presence of the telomere. These extra portions should be deleted from hg38 reference. 3q is an example of an arm that has additional sequences beyond the current reference end.

Table 1 summarizes the detailed comparison between the mapping results and hg38 reference for each chromosome arm. The range in number of genomes per arm is due to some genome assemblies not containing a consensus contig in the distal 500kb region of a chromosome arm. In addition, 5q, 13q, 15q, and 20p have more than 154 genomes, due to some genomes having two contigs (i.e., two long-range subtelomeric haplotypes) for an arm in a diploid genome. Table one also includes the current sizes of telomere-adjacent gaps designated in the HG38 reference sequence and the range the contig maps extended beyond that. Differences in telomere-adjacent gap sizes less than 10kb are unable to be distinguished and are estimated as 0. A negative number indicates there is excessive gap size, a positive number indicates insufficient gap size. For 1p and 17p the HG38 reference seems very inaccurate regardless of indicated gap size.

Table 1. Summary of Chromosomes

Chr Arm	Samples Represented	Large-scale Var[1]	Hg38 Tel-adj Gap[2] (kb)	Map Extension[3] (kb)	Chr Arm	Samples Represented	Large-scale Var[1]	Hg38 Tel-adj Gap[2] (kb)	Map Extension[3] (kb)
1p	113	High	inaccurate	N/A	1q	144	Low	10	0
2p	130	Low	10	0	2q	133	High	10	0-45
3p	143	Low	10	0	3q	110	High	60	70-140
4p	124	Low	10	0	4q[5]	133	N/A	10	N/A
5p	152	Low	10	0	5q	150	High	60	-60
6p	119	High	60	0	6q	146	High	60	-60
7p	104	High	10	100-175	7q	142	High	10	0
8p	153	High	60	-60	8q	151	Low	60	-20
9p	136	High	10	5-55	9q	128	High	60	-40-20
10p	146	Low	10	0	10q[5]	151	N/A	10	N/A
11p	121	High	60	0-80	11q	137	Low	10	-15
12p	145	Low	10	0	12q	147	Low	10	-20
13p	N/A	N/A	N/A	N/A	13q	152	Low	10	0
14p	N/A	N/A	N/A	N/A	14q	95	High	160	-160
15p	N/A	N/A	N/A	N/A	15q	140	High	10	0
16p[4]	153	Low	10	-10	16q	121	High	110	-20
17p[4]	127	Low	inaccurate	N/A	17q	124	High	10	-20
18p	144	Low	10	0	18q	150	Low	110	-110
19p	119	High	60	10	19q[4]	150	Low	10	0
20p	135	High	60	30-70	20q	148	Low	110	-70
21p	N/A	N/A	N/A	N/A	21q	115	Low	10	0
22p	N/A	N/A	N/A	N/A	22q[4]	153	Low	10	0
X/Yp	33	Low	10	N/A	X/Yq	139	Low	10	0

Caption: Table 1 contains the number of contigs from the 154 genomes present in each arm, the current amount of Ns in the hg38 reference padding, the range of the map extension lengths (if any), and the classification of each arm as High or Low variability. This is determined by looking at the total number of genomes for an arm, and how many were the majority haplotype vs the minor. If the minor haplotype was less than 10% the total, the arm is considered low variability. The acrocentric arms 13p, 14p, 15p, 21p, 22p cannot be determined due to the lack of reference. 4q and 10q have a known repeat D4Z4 in the subtelomeric region and are also excluded (43). For differences in reference gap and contig length being less than 10kb it is unable to be determined precisely and is estimated as 0. A negative number indicates the gap

estimated in the reference is longer than seen in the arm and a positive number indicates the arm is longer than the gap estimated. For 1p and 17p the HG38 reference is very inaccurate.

Superscripts:

1- If the minor haplotype was less than 10% the total haplotypes for the arm, the arm is considered low variability.

2 - The reference is inaccurate to the point where the size of the telomere adjacent gap of the reference cannot be evaluated

3 - For gap differences of <10kb, accuracy is unclear. These arms appear to be within the correct size range. N/A refers to arms that could not accurately be judged, including the acrocentric arms 13p, 14p, 15p, 21p, 22p. In addition, 4q and 10q contain a known D4Z4 repeat leading to widely variable ranges (35).

4 -contain INP sites, and this may affect data that could determine high vs low variability.

5 – Can be considered high variability with respect to high levels of large D4Z4 tandem repeat variability in the populations.

Population structure of paralogy blocks in subtelomeric regions

We used the consensus Bionano maps to identify subtelomeric paralogy blocks based upon the similarity of their nicking patterns to representative paralogy blocks defined first by Linardopoulou et al. and then extended by Stong et al. (24, 26). We then explored the population structure of specific subtelomeric paralogy blocks and combinations of adjacent subtelomeric paralogy blocks on each chromosome arm in the 154 genomes at the super-population level; 42 Africans (AFR), 30 Ad Mixed Americans (AMR), 30 East Asians (EAS), 24 Europeans (EUR) and 28 South Asians (SAS) (31).

Paralogy blocks 3, 5 and 9 are each relatively large and have distinct nick-labeling patterns generated by using the nicking enzyme Nt.BspQ1. Some smaller paralogy blocks lack a Nt.BspQ1 nicking site or have only a few, but consistently occur adjacent to and in the same orientation with other small blocks; in these cases we combined paralogy blocks to identify distinctive nicking patterns. Thus, combined blocks 1-2, 6-7-8, and 10-25-11-12 were analyzed

as three distinctive segments. Fig 4 shows the distribution of paralogy blocks 3, 5, 9, and 1-2 on chromosome arms 15q, 16q and 9q.

Block 3 has an uneven distribution between super populations, with its occurrence being chromosome- and population-dependent. Chromosome arms 3q, 6q, 15q, and 19p show a higher prevalence of block 3 in the majority of people with similar frequencies among super populations. Chromosome arms 2q, 5q, 6p, 7p, 8p, 9q, and 16q have lower prevalence of block 3 among all super populations. Arm 16q is statistically ($p<0.05$, Bonferroni correction) lower in the African super population compared to the other 4 super populations. Table S1 contains a detailed breakdown of the frequency of this block. This confirms the previous analysis of cosmid f7501 (with DNA sequence nearly identical to a portion of block 2 and half of block 3) by Trask et al, where fluorescence in situ hybridization localized the sequence on almost all genomes for 3q, 15q, 19p and only on a few genomes for 7p from African pygmy tribes (39). Block 3 is commonly found with Block 1 and 2. Block 1 and 2 show similar trends as block 3 on arm 16q, where block 1-2 is significantly more common in the African super population than the other super populations. Block 1-2 is found in just 3 genomes for chromosome arm 8p, all belonging to the African super population (Table S1), but it is not statistically different than other super populations.

Block 5 also has an uneven distribution between super populations (Fig 4). Block 5 has higher prevalence on chromosome arms 3q, 5q, 6p, 6q, 8p, 11p, and 15q with similar distributions between super populations (Table 2). However, block 5 has higher distribution on chromosome arms 9q and 16q in the AFR super population. Our results support the findings of previous studies of this paralogy block that could signify recent human divergence (39). Block 5 may have only spread to 9q and 16q in African populations after the other ancestral populations left Africa, resulting in its appearance there primarily in African populations. Alternatively, it may have spread to these arms prior to the divergence but became reduced in frequency in non-African populations due to genetic drift in those populations that left.

Table 2. Distribution of Block 5 by Population

Block 5	AFR with Block 5 / Total AFR maps	AMR with Block 5 / Total AMR maps	EAS with Block 5 / Total EAS maps	EUR with Block 5 / Total EUR maps	SAS with Block 5 / Total SAS maps
2q	0%	0%	0%	0%	4%
3q	54%	61%	76%	65%	35%
5q	88%	90%	97%	92%	82%
6p	56%	41%	21%	22%	32%
6q	83%	77%	62%	78%	80%
7p	7%	0%	0%	3%	7%
8p	81%	81%	67%	88%	78%
9q	62%	30%	48%	32%	15%
11p	49%	42%	21%	43%	35%
15q	93%	97%	97%	92%	93%
16q	14%	0%	0%	0%	4%
19p	10%	27%	47%	18%	19%

Caption: Table 2 shows the frequency of Block 5 on different chromosomes (rows) for each super population (column). AFR stands for the Africa super population category, AMR for Ad Mixed American, EAS for East Asian, EUR for European, and SAS for South Asian. Based on the Stong reference block 5 had previously been found on 5q, 6p, 6q, 8p, 11p, 15q, and 19p. In our dataset it was also found on 2q, 3q, 7p, 9q, and 16q.

Blocks group 9, group 6-7-8, and group 10-25-11-12 do not show any statistically significant differences in frequencies between super populations.

Arms including 3q, 2q, 9p, 9q, 11p, 15q, 17p, and 19p have additional extended regions compared to the HG38 reference. These extended regions don't belong to any known paralogy blocks. These could represent new combinations of existing subtelomeric segmental duplication material, or subtelomeric insertions of material from elsewhere in the genome. Most of the arms show even distributions of the extended regions between super populations, except arms 17p and 9p. These two arms have extra extensions only in AFR super population, but with relatively low frequencies.

At the super population level, in general, paralogy blocks are present at equal frequency on all five super-populations on most of the chromosome arms that contain the paralogy blocks. However, a few chromosome arms show significantly different frequencies of paralogy blocks (blocks 1-5 and additional extended regions beyond the HG38 reference) in the African super-population. These paralogy blocks are DNA segments immediately adjacent to the telomere, which may be associated with their relatively rapid duplication and spread amongst multiple human subtelomeres.

DISCUSSION

In this study we utilized optical mapping (27, 40) for 154 individual genomes. We used long DNA molecules (>150kb) and a minimum coverage depth of 60x for each genome. For each genome, every chromosome arm was compared with the hg38 reference and the Stong subtelomeric reference (24). The current hg38 reference contains telomere-adjacent gaps represented by strings of “N”s corresponding to missing base pairs in the reference. Our data shows that these telomere-adjacent gaps are frequently inaccurate and represent both structural variations as well as sequence gaps. Like our previous 6 sample study, we were able to detect new long range haplotypes (22); here we created a much more comprehensive catalog of these alternative haplotypes and their relative frequencies in different populations. 18 chromosome arms (1p, 2q, 3q, 5q, 6p, 6q, 7p, 7q, 8p, 9p, 9q, 11p, 14q, 15q, 16q, 17q, 19p, 20p) are classified as highly variable (minor haplotypes comprised more than 10% of the total genomes). 18 other chromosome arms (1q, 2p, 3p, 4p, 4q, 5p, 8q, 10p, 10q, 11q, 12p, 12q, 13q, 18p, 18q, 20q, 21q, XqYq) showed minimal variations compared to the hg38 reference sequences.

Specific subtelomeres from some genomes failed to assemble and/or map to the reference genome. The reason for this is unclear. These failures may be due to problems of

short molecule lengths or low labeling density causing samples to form shorter contigs than normal. The individual genomes missing subtelomere assemblies were not consistent, precluding non-specific DNA fragmentation in certain samples as the cause for these failures to assemble.

Using these mapping data, we also examined the distribution of the Stong reference paralogy blocks between the 5 super populations. Block group 1-2, block 3, and block 5 showed a statistically significant prevalence on chromosome arm 16q, in the AFR super population over the other super populations. There is not a significant difference on other arms or in the other blocks.

Some genomes had haplotypes with extension beyond the hg38 reference which did not match any known block in the Stong reference. These also seemed to be more prevalent AFR super population, as the others did not contain the unknown block extension. However, this novel extension in AFR was not statistically significant, possibly due to the small sample size.

From this dataset, we can speculate on the timeline of the development of the paralogy blocks in subtelomeric regions based on their distribution between super populations. In the case of block 3, it is very common on 3 arms, rare on 3 other chromosomes and not found on the rest. Chromosome arms 3q, 15q, and 19p show heavy prevalence of block 3 with a majority of people in all populations having the block, so block 3 may have spread to these arms first and later in 3 chromosome arms (7p, 16p, 16q) where only a few genomes have block 3. Only 16q was significantly different than the other blocks. These distribution differences could be attributed to human migration out of Africa. The development of block 3 on 3q, 15q and 19p likely predates the migration and subsequent expansion of human populations out of Africa (41). 7p, 16p and 16q potentially developed their instance of block 3 after the initial migration, and spread to all populations remaining in Africa. Alternatively, it may have existed but not yet become a fixed allele at the time of migration and lost over time to genetic drift, and thus not be found in non-African populations. However, arms 2q, 5q, 6p, and 8p do not share this

445 segregation, as their block 3 is present in small frequencies (<10%) and evenly distributed
446 among super populations. The reasons for this even distribution are unknown. It could be that
447 the mechanisms of subtelomeric diversity have led to each of these populations simultaneously
448 developing them independently. The exact mechanisms of subtelomeric variation remains
449 undetermined. Overall, these results support the findings of a previous study of paralogy block
450 3 that used 8 isolated ethnic groups (2 Pygmy groups, Melanesian, 2 Amerindian, Khmer, Druze
451 and Caucasian, 45 total genomes) and 8 primate genomes, that signifies a recent human
452 divergence (39).

453 Other paralogy block groups, such as block group 6-7-8, showed different trends, where
454 a majority of all populations had the block and there were no statistically significant difference
455 between super populations for any arm. These blocks are likely to have developed and spread
456 to the arms earlier than the unevenly distributed blocks.

457 This work catalogs a large number of novel long-range subtelomere haplotypes and
458 determines their frequencies and contexts in terms of specific subtelomeric duplicons on each
459 chromosome arm. This information will provide mapping guideposts for their eventual sequence
460 determination, and helps to clarify the currently ambiguous nature of many specific subtelomere
461 structures as represented in the current reference sequence (HG38). As such, this information
462 is an essential step in understanding the impact of subtelomeric cis-sequences on transcription
463 of TERRA and other functional subtelomeric RNAs and their roles in regulating single-telomere
464 lengths and function, as well as delineating the population structure and evolution of highly
465 variable human subtelomere regions.

466

467 **Methods:**

468 **High molecular weight DNA extraction.**

469 Mammalian cells were embedded in gel plugs and High Molecular Weight DNA was purified as
470 described in a commercial large DNA purification kit (BioRad #170-3592). Plugs were incubated

with lysis buffer and proteinase K for four hours at 50°C. The plugs were washed and then solubilized with GELase (Epicentre). The purified DNA was subjected to four hours of drop-dialysis. It was quantified using Quant-iTdsDNA Assay Kit (Life Technology), and the quality was assessed using pulsed-field gel electrophoresis.

DNA labeling.

The DNA was labeled with nick-labeling (42) as described previously using the IrysPrep Reagent Kit (BioNano Genomics). Specifically, 300 ng of purified genomic DNA was nicked with 7 U nicking endonuclease Nt.BspQI (New England BioLabs, NEB) at 37°C for two hours in NEB Buffer 3.1. The nicked DNA was labeled with a fluorescent-dUTP nucleotide analog using Taq polymerase (NEB) for one hour at 72°C. After labeling, the nicks were ligated with Taq ligase (NEB) in the presence of dNTPs. The backbone of fluorescently labeled DNA was stained with YOYO-1 (Invitrogen).

A subset of the samples were labeled using the newer Direct Label Enzyme (DLE) method (Bionano Genomics). These samples used the DNA Labeling Kit-DLS 80005 and followed the manufacturer's instructions. In Summary, 750ng of the gDNA was labeled using DLE-1 enzyme and reaction mix followed by Proteinase K digestion (Qiagen). The DNA back bone was stained after drop dialysis. The stained sample was then homogenized and incubated at room temperature over nigh before quantified using Qubit dsDNA HS Kit (Invitrogen).

Data collection.

The DNA was loaded onto the nano-channel array of BioNano Genomics IrysChip by electrophoresis of DNA. Linearized DNA molecules were imaged using a custom made whole genome mapping system. The DNA backbone (outlined by YOYO-1 staining) and locations of fluorescent labels along each molecule were detected using an in-house image detection software. The set of label locations relative to the DNA backbone for each DNA molecule

defines an individual single-molecule map. A commercial version of this whole-genome mapping and imaging system (Irys) is available from Bionano Genomics.

De novo genome map assembly.

Single-molecule maps were assembled *de novo* into consensus maps using software tools developed at BioNano Genomics, specifically Refaligner and Assembler (1). Briefly, the assembler is a custom implementation of the overlap-layout-consensus paradigm with a maximum likelihood model. An overlap graph was generated based on pairwise comparison of all molecules as input. Redundant and spurious edges were removed. The assembler outputs the longest path in the graph and consensus maps were derived. Consensus maps are further refined by mapping single molecule maps to the consensus maps and label positions are recalculated. Refined consensus maps are extended by mapping single molecules to the ends of the consensus and calculating label positions beyond the initial maps. After merging of overlapping maps, a final set of consensus maps was output and used for subsequent analysis. The map assemblies are very robust to the relatively small errors in labeling (10% false positive, due to extra nickings at wrong sites, and 10% false negative, due to missing nicks). This does not affect the maps and haplotype calls as the haplotypes are both are based on multiple nicking sites and multiple single molecules.

Block Definition.

Subtelomeric paralogy blocks originally defined by Linardopoulou et al and extended/refined by Stong et al., (24, 26) are sequence segments of highly similar duplicated subtelomeric DNA that can be identified as discrete contiguous duplicated DNA segments in subtelomere reference assemblies(24). Paralogy blocks were characterized for mapping purposes by the pattern of nick sites in the representative sequenced reference paralogy block or set of adjacent paralogy blocks. These nicking patterns were then compared with the subtelomere regions of maps

generated for each genome. Block boundaries were identified by a qualitative comparison based on the distance between nick sites and their pattern on several arms with shared blocks.

Statistical analysis of paralogy blocks in super population

An analysis of variant (ANOVA) was calculated on the block presence per genome, grouped by super population. A Bonferroni correction was then performed to determine significance between the 4 super populations. This statistical analysis was repeated independently for each paralogy block or block group analyzed.

SUPPLEMENTARY DATA

Available online

ACKNOWLEDGEMENTS

Part of the informatics analysis was run on hardware supported by Drexel's University Research Computing Facility. We thank Bionano Genomics Inc. for assistance in data generation and bioinformatics support.

FUNDING

R01HG005946 (MX and PYK). R21CA177395 (MX and HR), R01CA140652 (HR).

REFERENCES

1. Azzalin CM, Reichenbach P, Khoriauli L, Giulotto E, Lingner J. Telomeric repeat containing RNA and RNA surveillance factors at mammalian chromosome ends. Science. 2007;318(5851):798-801.
2. Porro A, Feuerhahn S, Delafontaine J, Riethman H, Rougemont J, Lingner J. Functional characterization of the TERRA transcriptome at damaged telomeres. Nature Communications. 2014;5.
3. Porro A, Feuerhahn S, Reichenbach P, Lingner J. Molecular Dissection of Telomeric Repeat-Containing RNA Biogenesis Unveils the Presence of Distinct and Multiple Regulatory Pathways. Molecular and Cellular Biology. 2010;30(20):4808-17.
4. Deng Z, Norseen J, Wiedmer A, Riethman H, Lieberman PM. TERRA RNA Binding to TRF2 Facilitates Heterochromatin Formation and ORC Recruitment at Telomeres. Molecular Cell. 2009;35(4):403-13.
5. Chu H-P, Cifuentes-Rojas C, Kesner B, Aeby E, Lee H-G, Wei C, et al. TERRA RNA Antagonizes ATRX and Protects Telomeres. Cell. 2017;170(1):86-101.e16.
6. Britt-Compton B, Rowson J, Locke M, Mackenzie I, Kipling D, Baird DM. Structural stability and chromosome-specific telomere length is governed by cis-acting determinants in humans. Human Molecular Genetics. 2006;15(5):725-33.
7. Graakjaer J, Bischoff C, Korshohn L, Holstebroe S, Vach W, Bohr VA, et al. The pattern of chromosome-specific variations in telomere length in humans is determined by inherited, telomere-near factors and is maintained throughout life. Mechanisms of Ageing and Development. 2003;124(5):629-40.
8. Graakjaer J, Der-Sarkissian H, Schmitz A, Bayer J, Thomas G, Kolvraa S, et al. Allele-specific relative telomere lengths are inherited. Human Genetics. 2006;119(3):344-50.
9. Nergadze SG, Farnung BO, Wischnewski H, Khoriauli L, Vitelli V, Chawla R, et al. CpG-island promoters drive transcription of human telomeres. Rna-a Publication of the Rna Society. 2009;15(12):2186-94.
10. Caslini C, Connelly JA, Serna A, Broccoli D, Hess JL. MLL Associates with Telomeres and Regulates Telomeric Repeat-Containing RNA Transcription. Molecular and Cellular Biology. 2009;29(16):4519-26.
11. Deng Z, Campbell AE, Lieberman PM. TERRA, CpG methylation and telomere heterochromatin Lessons from ICF syndrome cells. Cell Cycle. 2010;9(1):69-74.
12. Yehezkel S, Segev Y, Viegas-Pequignot E, Skorecki K, Selig S. Hypomethylation of subtelomeric regions in ICF syndrome is associated with abnormally short telomeres and enhanced transcription from telomeric regions. Human Molecular Genetics. 2008;17(18):2776-89.
13. Kermouni A, Vanroost E, Arden KC, Vermeesch JR, Weiss S, Godelaine D, et al. THE IL-9 RECEPTOR GENE (IL9R) - GENOMIC STRUCTURE, CHROMOSOMAL LOCALIZATION IN THE PSEUDOAUTOSOMAL REGION OF THE LONG ARM OF THE SEX-CHROMOSOMES, AND IDENTIFICATION OF IL9R PSEUDOGENES AT 9QTER, 10PTER, 16PTER, AND 18PTER. Genomics. 1995;29(2):371-82.
14. Linardopoulou EV, Parghi SS, Friedman C, Osborn GE, Parkhurst SM, Trask BJ. Human subtelomeric WASH genes encode a new subclass of the WASP family. Plos Genetics. 2007;3(12):2477-85.
15. Linardopoulou E, Mefford HC, Nguyen O, Friedman C, van den Engh G, Farwell DG, et al. Transcriptional activity of multiple copies of a subtelomerically located olfactory receptor gene that is polymorphic in number and location. Human Molecular Genetics. 2001;10(21):2373-83.
16. Mah N, Stoehr H, Schulz HL, White K, Weber BHF. Identification of a novel retina-specific gene located in a subtelomeric region with polymorphic distribution among multiple human chromosomes. Biochimica Et Biophysica Acta-Gene Structure and Expression. 2001;1522(3):167-74.
17. Riethman H, Ambrosini A, Castaneda C, Finklestein J, Hu XL, Mudunuri U, et al. Mapping and initial analysis of human subtelomeric sequence assemblies. Genome Research. 2004;14(1):18-28.

589 18. Cabianca DS, Casa V, Bodega B, Xynos A, Ginelli E, Tanaka Y, et al. A long ncRNA links copy
590 number variation to a polycomb/trithorax epigenetic switch in FSHD muscular dystrophy. Cell.
591 2012;149(4):819-31.
592 19. Lou Z, Wei J, Riethman H, Baur JA, Voglauer R, Shay JW, et al. Telomere length regulates ISG15
593 expression in human cells. Aging-Us. 2009;1(7):608-21.
594 20. Robin JD, Ludlow AT, Batten K, Magdinier F, Stadler G, Wagner KR, et al. Telomere position
595 effect: regulation of gene expression with progressive telomere shortening over long distances. Genes &
596 Development. 2014;28(22):2464-76.
597 21. Church DM, Schneider VA, Graves T, Auger K, Cunningham F, Bouk N, et al. Modernizing
598 Reference Genome Assemblies. PLOS Biology. 2011;9(7):e1001091.
599 22. Young E, Pastor S, Rajagopalan R, McCaffrey J, Sibert J, Mak AC, et al. High-throughput single-
600 molecule mapping links subtelomeric variants and long-range haplotypes with specific telomeres.
601 Nucleic acids research. 2017.
602 23. Riethman H. Human subtelomeric copy number variations. Cytogenet Genome Res. 2008;123(1-
603 4):244-52.
604 24. Stong N, Deng Z, Gupta R, Hu S, Paul S, Weiner AK, et al. Subtelomeric CTCF and cohesin binding
605 site organization using improved subtelomere assemblies and a novel annotation pipeline. Genome
606 Research. 2014;24(6):1039-50.
607 25. Kidd JM, Cooper GM, Donahue WF, Hayden HS, Sampas N, Graves T, et al. Mapping and
608 sequencing of structural variation from eight human genomes. Nature. 2008;453(7191):56-64.
609 26. Linardopoulou EV, Williams EM, Fan Y, Friedman C, Young JM, Trask BJ. Human subtelomeres
610 are hot spots of interchromosomal recombination and segmental duplication. Nature. 2005;437.
611 27. Lam ET, Hastie A, Lin C, Ehrlich D, Das SK, Austin MD, et al. Genome mapping on nanochannel
612 arrays for structural variation analysis and sequence assembly. Nature Biotechnology. 2012;30(8):771-6.
613 28. Mak ACY, Lai YYY, Lam ET, Kwok T-P, Leung AKY, Poon A, et al. Genome-Wide Structural
614 Variation Detection by Genome Mapping on Nanochannel Arrays. Genetics. 2015.
615 29. Alkan C, Sajjadian S, Eichler EE. Limitations of next-generation genome sequence assembly. Nat
616 Methods. 2011;8(1):61-5.
617 30. Riethman HC, Xiang Z, Paul S, Morse E, Hu XL, Flint J, et al. Integration of telomere sequences
618 with the draft human genome sequence. Nature. 2001;409(6822):948-51.
619 31. Levy-Sakin M, Pastor S, Mostovoy Y, Li L, Leung AKY, McCaffrey J, et al. Genome maps across 26
620 human populations reveal population-specific patterns of structural variation. Nature Communications.
621 2019;10(1):1025.
622 32. McCaffrey J, Young E, Lassahn K, Sibert J, Pastor S, Riethman H, et al. High-throughput single-
623 molecule telomere characterization. Genome research. 2017;27(11):1904-15.
624 33. Macina RA, Negorev DG, Spais C, Ruthig LA, Hu XL, Riethman HC. SEQUENCE ORGANIZATION OF
625 THE HUMAN-CHROMOSOME 2Q TELOMERE. Human Molecular Genetics. 1994;3(10):1847-53.
626 34. Inglehearn CF, Cooke HJ. A VNTR immediately adjacent to the human pseudoautosomal
627 telomere. Nucleic acids research. 1990;18(3):471-6.
628 35. Brown WR. A physical map of the human pseudoautosomal region. EMBO J. 1988;7(8):2377-85.
629 36. Genomics B. Bionano Prep Direct Label and Stain (DLS) Protocol 2018 [Available from:
630 https://bionanogenomics.com/wp-content/uploads/2018/04/30206-Bionano-Prep-Direct-Label-and-
631 Stain-DLS-Protocol.pdf.
632 37. Wilkie AOM, Higgs DR, Rack KA, Buckle VJ, Spurr NK, Fischel-Ghodsian N, et al. Stable length
633 polymorphism of up to 260 kb at the tip of the short arm of human chromosome 16. Cell.
634 1991;64(3):595-606.
635 38. Xiang Z, Hu XL, Flint J, Riethman HC. A Sequence-Ready Map of the Human Chromosome 17p
636 Telomere. Genomics. 1999;58(2):207-10.

637 39. Trask BJ, Friedman C, Martin-Gallardo A, Rowen L, Akinbami C, Blankenship J, et al. Members of
638 the olfactory receptor gene family are contained in large blocks of DNA duplicated polymorphically near
639 the ends of human chromosomes. Human Molecular Genetics. 1998;7(1):13-26.
640 40. Hastie AR, Dong L, Smith A, Finklestein J, Lam ET, Huo N, et al. Rapid Genome Mapping in
641 Nanochannel Arrays for Highly Complete and Accurate De Novo Sequence Assembly of the Complex
642 Aegilops tauschii Genome. Plos One. 2013;8(2).
643 41. Mefford HC, Trask BJ. The complex structure and dynamic evolution of human subtelomeres.
644 Nature Reviews Genetics. 2002;3:91+.
645 42. Xiao M, Phong A, Ha C, Chan T-F, Cai D, Leung L, et al. Rapid DNA mapping by fluorescent single
646 molecule detection. Nucleic acids research. 2007;35(3).
647 43. Zeng W, Chen Y-Y, Newkirk DA, Wu B, Balog J, Kong X, et al. Genetic and Epigenetic
648 Characteristics of FSHD-Associated 4q and 10q D4Z4 that are Distinct from Non-4q/10q D4Z4 Homologs.
649 Human Mutation. 2014;35(8):998-1010.

650

651

652

Figure Captions:

Figure 1. Example of a long-range haplotype in subtelomeric regions supported by single molecule evidence

Caption: Colored rectangles represent paralogy blocks defined in the subtelomere assemblies of Stong et al. (2014). The blue bar shows the hg38 reference with Nt.BsPQ1 nick sites as dark blue dashes along it. The yellow bar shows the consensus contig for this sample, with dark green marks indicating a match to the reference and lighter green/blue showing nick sites without a reference match. The colored rectangles about the yellow bar show the paralogy blocks that match the pattern seen in the extended region. The brown rows indicate single molecules, which extend well past the block regions and into the single copy region. A teal arrow shows the distance, 70kb, from the telomere as defined by the Bionano single-molecule maps to the end of the HG38 reference assembly. A black arrow represents 60 kb of unknown sequence currently in the HG38 reference as 'N', an estimate of gap size to the end of the chromosome. Dashed boxes on top of the molecules indicate portions of the extended region that match to paralogy blocks 1-5 but are not in the current references for 3q. A red T indicates the telomeric end of the 3q map.

Figure 2. Major haplotypes for highly variable arms.

Caption: The Stong et al. assembly blocks are shown as colored rectangles above blue Bionano genome mapping bars. Yellow rows with green ticks show haplotypes below these. A teal arrow indicates the size of additional extended regions not covered by the reference. A black arrow represents unknown sequence currently in the HG38 reference as 'N', an estimate of gap size to the end of the chromosome. If the black arrow is dashed it signifies a region of unknown telomere-adjacent gap sequence that should be deleted. A red T indicates the Stong 2014 assembly reached the telomere, and the lack of one means that assembly was unable to reach the telomere repeats. Each highly variable arm is included here. Figure 2A shows 1p, 2q, and 3q. Figure 2B shows 5q, 6p, and 6q. Figure 2C shows arms 7p, 7q, and 8p. Figure 2D shows 9p, 9q and 11p. Figure 2E illustrates 14q, 15q, 16q and Figure 2F has arms 17q, 19p and 20p.

Figure 3. Telomere Labeling Shows sizes of telomere-adjacent gaps in subtelomeres.

Caption: Blue bars represent the nick sites in hg38 reference. Yellow bars with green Nt.BsPQ1 nick sites represent the main haplotype seen in the genomes. A black dashed arrow indicated the width of the telomere-adjacent gap sequence that should be deleted from the hg38 reference. An image below the haplotype shows a single telomere labeled molecule confirming the end of the chromosome arm. These telomeres were labeled using CRISPR-Cas9 to tag the telomere repeat and incorporate a fluorophore(32). None of the subtelomeric haplotypes for each of these arms extends past the telomere label shown here.

Figure 4. Distribution of Paralogy Block 5 in 15q, 16q and 9q.

Caption: The solid color rectangle bars show the paralogy blocks defined in the subtelomeric assemblies of Stong et al. (2014). The narrow grey line segments to the right of the colored blocks show the single-copy DNA region. Blue rectangles with dark blue lines show the HG38 reference with Nt.BsPQ1 nick sites. Paralogy block five is shown as a dashed blue rectangle on top of yellow rows representing consensus maps for particular genomes. Additional

paralogy blocks are also shown as dashed colored rectangles. A teal arrow indicates the size of additional extended regions not covered by the reference. A black arrow represents unknown sequence currently in the HG38 reference as 'N', an estimate of gap size to the end of the chromosome. If the black arrow is dashed it signifies a region of unknown telomere-adjacent gap sequence that should be deleted.

Supporting Information Legends:

Fig S1-S7: Comprehensive Analysis of Human Subtelomeres by Whole Genome Mapping

S1-S7 Caption: Supplemental figures S1 through S7 show the major haplotypes for each chromosome arm in the less variable set of subtelomeres. The Stong Assembly paralogy blocks are shown as colored rectangles above blue Bionano optical mapping bars. Yellow rows with green ticks show haplotypes below these. A teal arrow indicates the size of additional extended regions not covered by the reference. A black arrow indicates the region indicated as a telomere-adjacent gap in the HG38 reference sequence. If the black arrow is dashed it signifies a region that should be deleted. Each low-variability arm is briefly described here.

Supplemental Table 1: Block Frequencies by Chromosome and Superpopulation.

Caption: Table S1 shows the frequency of Block 1-2, Block 3, Block 6-7-8, Block 9, and Blocks 10-11-25-12 on different chromosomes (rows) for each super population (column). AFR stands for the Africa super population category, AMR for Ad Mixed American, EAS for East Asian, EUR for European, and SAS for South Asian.

Figures:

Figure 1. Extended Haplotypes in subtelomeric regions of 3q in GM191025 supported by single molecule evidence

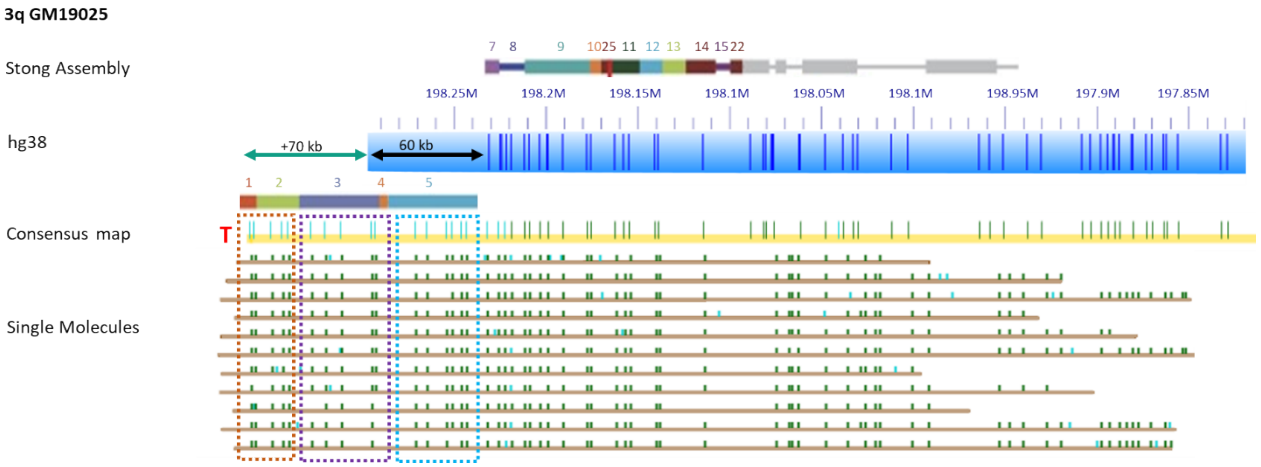

729 Figure 2. Major Haplotypes of Highly Variable Subtelomere Regions (A, B, C, D, E, F)
730

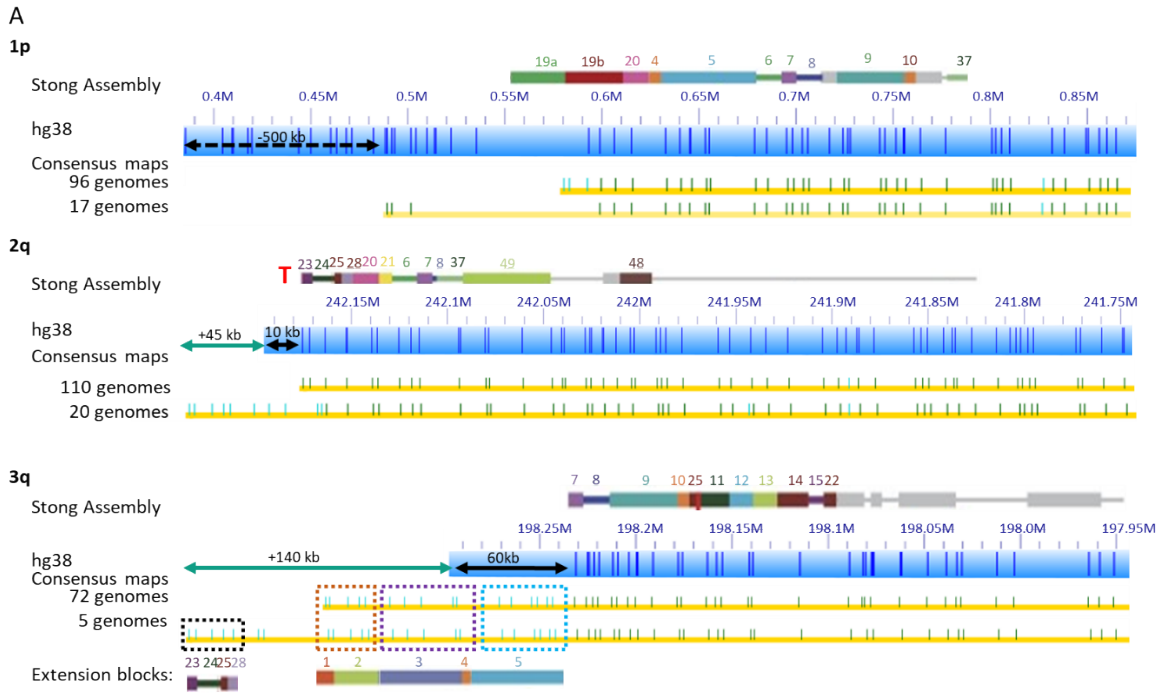

731
732

B

733
734

735
736

C

737
738

739
740

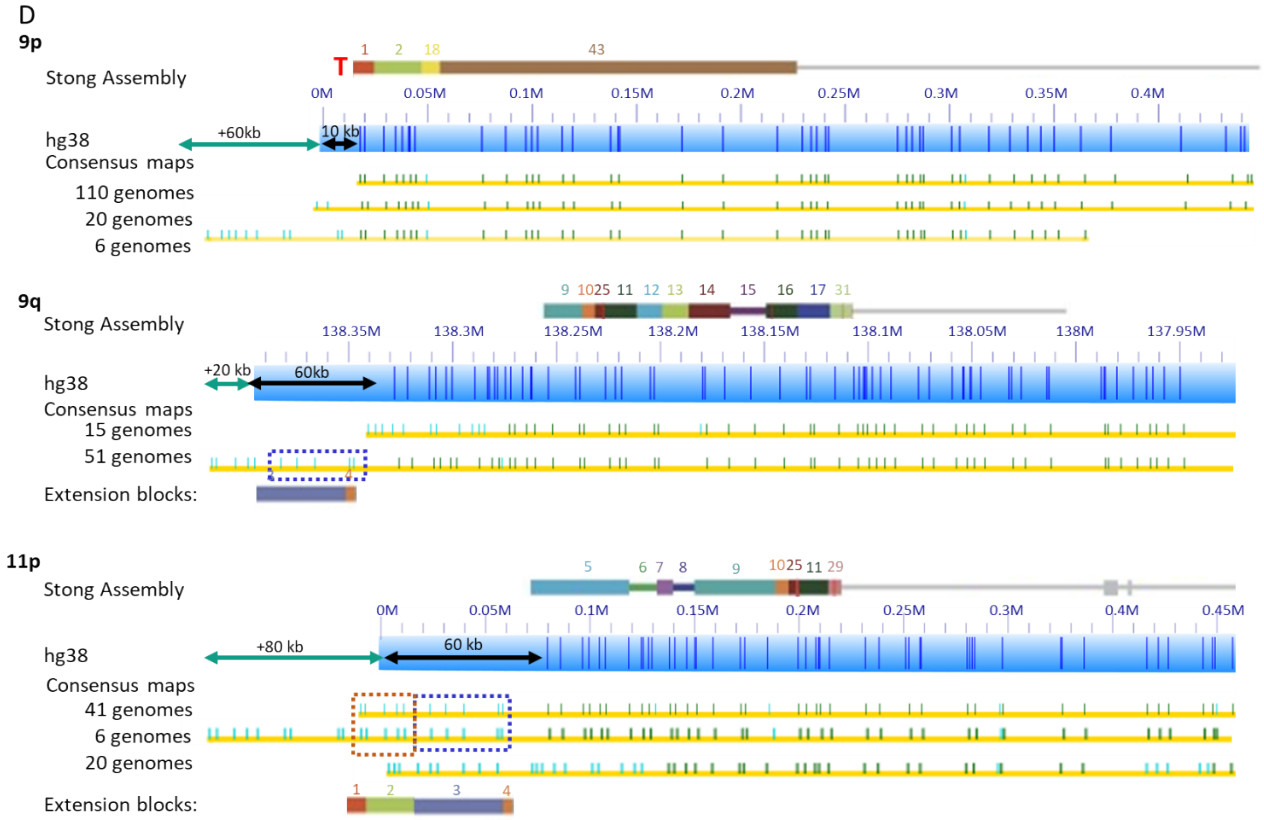

741
742

E

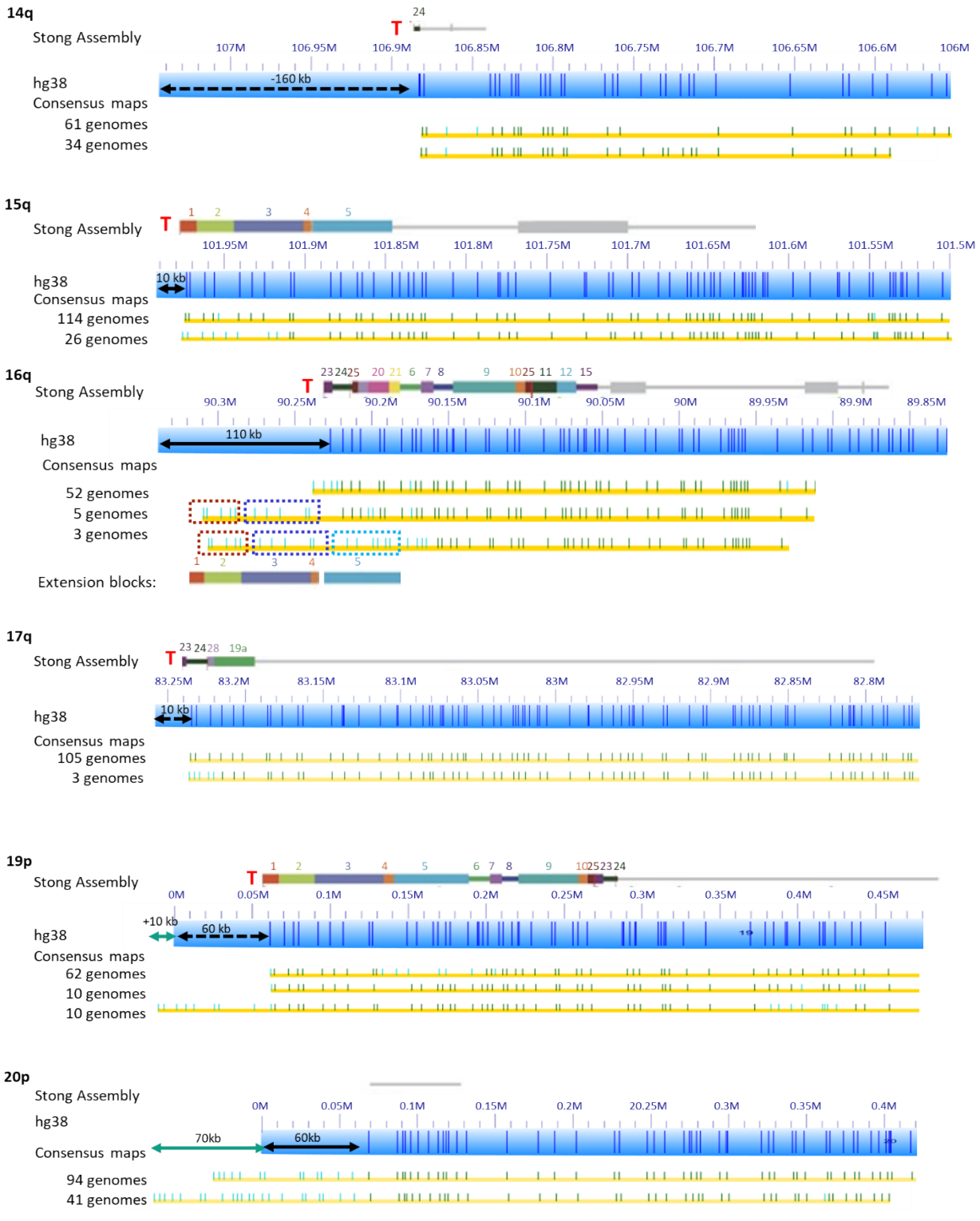

745 Figure 3. Telomere Labeling Shows Inaccurate Sizing of Telomere-adjacent Gap Segments in
746 HG38 Subtelomere Regions
747

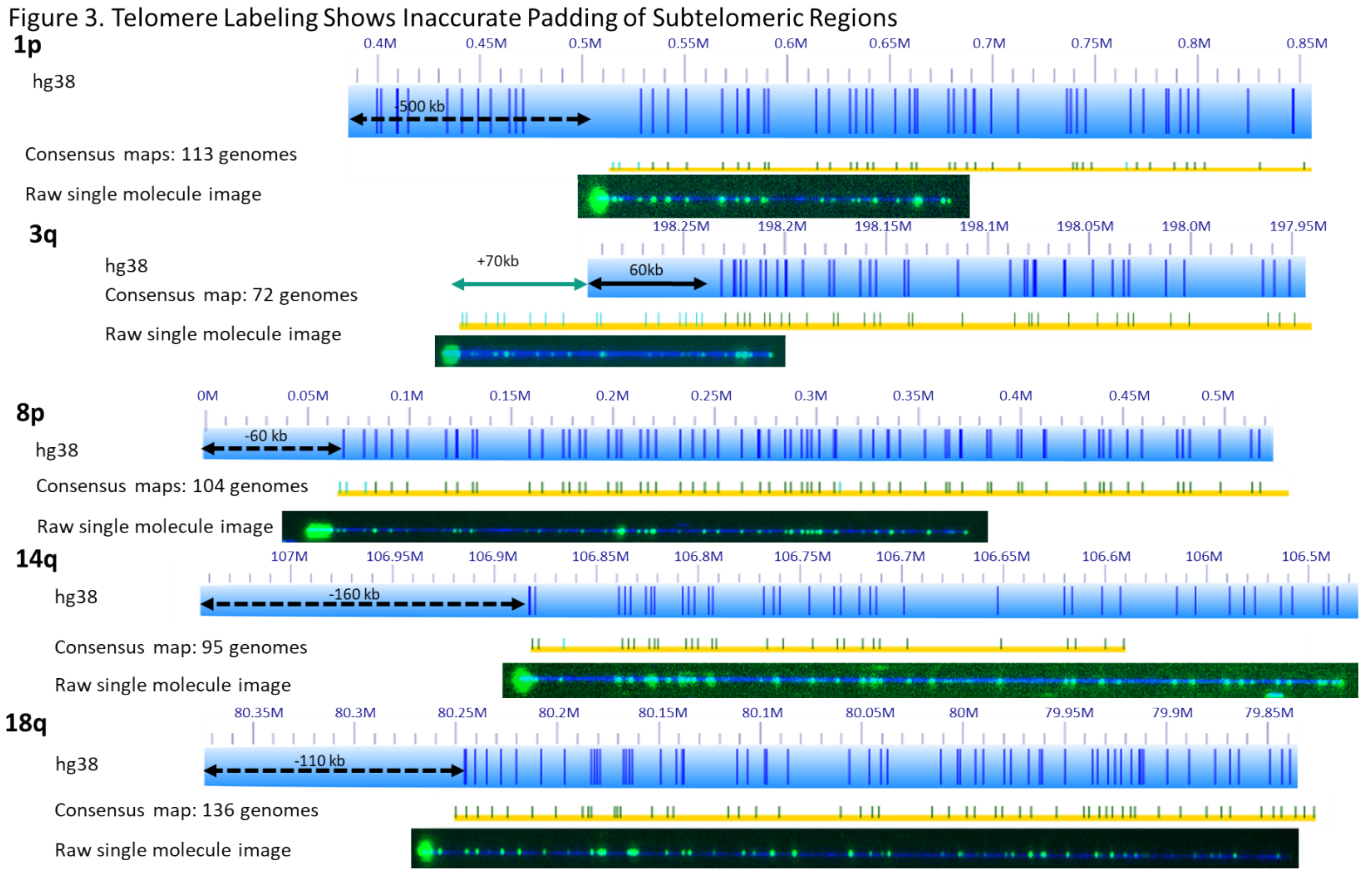

748
749

Figure 4. Distribution of Paralogy Block 5 in 15q, 16q and 9q.